Neuron
Article

Making Waves: Initiation and Propagation of Corticothalamic Ca^{2+} Waves In Vivo

Albrecht Stroh,[1,2,3] Helmuth Adelsberger,[1,2] Alexander Groh,[1] Charlotta Rühlmann,[1] Sebastian Fischer,[1] Anja Schierloh,[1] Karl Deisseroth,[4,5] and Arthur Konnerth[1,2,*]
[1]Institute of Neuroscience, Technical University Munich, Biedersteiner Strasse 29, 80802 Munich, Germany
[2]Munich Cluster for Systems Neurology (SyNergy) and Center for Integrated Protein Sciences Munich (CIPSM), Biedersteiner Strasse 29, 80802 Munich, Germany
[3]Institute for Microscopic Anatomy and Neurobiology, Focus Program Translational Neurosciences (FTN), Johannes Gutenberg-University Mainz, Hanns-Dieter-Hüsch-Weg 19, 55128 Mainz, Germany
[4]HHMI
[5]Department of Bioengineering
Stanford University, 318 Campus Drive West, Stanford, CA 94305, USA
*Correspondence: arthur.konnerth@lrz.tu-muenchen.de
http://dx.doi.org/10.1016/j.neuron.2013.01.031

SUMMARY

Corticothalamic slow oscillations of neuronal activity determine internal brain states. At least in the cortex, the electrical activity is associated with large neuronal Ca^{2+} transients. Here we implemented an optogenetic approach to explore causal features of the generation of slow oscillation-associated Ca^{2+} waves in the in vivo mouse brain. We demonstrate that brief optogenetic stimulation (3–20 ms) of a local group of layer 5 cortical neurons is sufficient for the induction of global brain Ca^{2+} waves. These Ca^{2+} waves are evoked in an all-or-none manner, exhibit refractoriness during repetitive stimulation, and propagate over long distances. By local optogenetic stimulation, we demonstrate that evoked Ca^{2+} waves initially invade the cortex, followed by a secondary recruitment of the thalamus. Together, our results establish that synchronous activity in a small cluster of layer 5 cortical neurons can initiate a global neuronal wave of activity suited for long-range corticothalamic integration.

INTRODUCTION

Slow oscillations of membrane potential in the frequency range below 1 Hz have been described in vivo both in neocortical and thalamic neurons (He, 2003; Steriade et al., 1993a, 1993b, 1993c). They are phase locked to population neuronal activity measured by electroencephalogram (EEG) and represent a characteristic feature of non-REM sleep (Wang, 2010). Slow oscillatory activity is associated with Up-Down state transitions in cortical neurons, consisting of hyperpolarized Down states and intermittent depolarized Up states, as indicated by experiments performed both in vivo (Doi et al., 2007) and in vitro (Shu et al., 2003). These brain state transitions play a major role in memory consolidation (Landsness et al., 2009; Rolls et al., 2011; Steriade and Timofeev, 2003) and may also control, at least in cortical slices, gamma activity (Compte et al., 2008). During non-REM sleep as well as during many forms of anesthesia, slow oscillations occur spontaneously (Haider et al., 2006), but they can also be evoked by brief sensory stimulation (Gao et al., 2009; Sakata and Harris, 2009), similar to activity patterns in early postnatal development such as spindle bursts (Hanganu et al., 2006; Khazipov et al., 2004). Furthermore, recent experimental evidence indicates that slow-wave-like activity is present both during periods of quiet wakefulness as well as in local neuronal clusters in nonanesthetized rodents (Poulet and Petersen, 2008; Vyazovskiy et al., 2011).

Up to now, slow oscillatory activity has been monitored on population level mostly by electrophysiological methods, such as electric local field potential (LFP) recordings (Steriade, 2006). However, it is becoming increasingly clear that LFP might integrate neuronal activity through volume conductance over many millimeters (Kajikawa and Schroeder, 2011; Lindén et al., 2011), thus not allowing for unambiguous comparisons of spatial dynamics of slow-wave activity at different locations. Previous studies show that fluorometric Ca^{2+} recordings of neural activity, which monitor predominantly action potential firing (Kerr et al., 2005; Stosiek et al., 2003), represent a useful method of recording slow-wave-associated Ca^{2+} transients (Rochefort et al., 2009). Such Ca^{2+} waves can be detected in vivo in the mammalian neocortex both during development (Adelsberger et al., 2005) and in the adult (Kerr et al., 2005). In development, these waves occur spontaneously in resting pups and may mirror functional organization of cortical circuits. In the adult, these waves may be associated with electrically recorded slow waves (Grienberger et al., 2012; Rochefort et al., 2009). Yet, the relation between Ca^{2+} waves and slow electrical waves on a global level remains unclear. Ca^{2+} waves in subcortical structures such as the thalamus have not been identified up to now.

There is evidence that both spontaneous as well as sensory-evoked slow oscillatory activity may represent traveling waves, recruiting large areas of the cortex (Ferezou et al., 2007; Massimini et al., 2004; Xu et al., 2007). Even though slow oscillation-associated activity eventually recruits all cortical layers, the onset of spontaneous activity is recorded first, both in vivo and in vitro, in layer 5 (Sakata and Harris, 2009; Sanchez-Vives and

McCormick, 2000), while sensory-evoked activity seems to originate in the thalamorecipient layer 4 (Sakata and Harris, 2009). The specific roles of the thalamus and the cortex in the generation and propagation of slow oscillations are still a matter of debate (Chauvette et al., 2010; McCormick et al., 2003; Wu et al., 2008). Early results point to the neocortex as generator, as the thalamic slow oscillations do not survive decortication (Timofeev and Steriade, 1996). Moreover, cortical slow oscillations persist both upon thalamic lesions as well as in cortical slice preparations (Constantinople and Bruno, 2011; Sanchez-Vives and McCormick, 2000; Steriade et al., 1993c). In thalamocortical slice preparations, thalamic stimulation can trigger cortical slow-wave-associated Up states; yet, the thalamus is not required for their generation (MacLean et al., 2005; Rigas and Castro-Alamancos, 2007). However, a recent study suggests a re-evaluation of the role of the thalamus, providing evidence for a critical role of two intrinsic thalamic oscillators, which may interact with a synaptically based cortical oscillator (Crunelli and Hughes, 2010). This work challenges the view that the cortex is causally involved in the generation of slow oscillations in vivo.

A way of causally probing the distinct roles of cortex and the thalamus involves the targeted manipulations of cortical and thalamic networks. Optogenetics can provide the tools necessary for a local and specific interrogation of neuronal circuitry (Gradinaru et al., 2010; Zhang et al., 2007). The use of optogenetics provided critical insights into the cell type-specific induction of gamma oscillations and its consequences on information flow (Sohal et al., 2009). However, in order to investigate initiation and long-range propagation of slow oscillatory activity, optogenetics needs to be combined with an effective technique to record network activity with sufficient temporal resolution and spatial specificity. In the present study, we monitored the Ca^{2+} transients associated with slow-wave activity by using mainly optic fiber-based fluorometric Ca^{2+} recordings (Adelsberger et al., 2005; Grienberger et al., 2012). For this purpose, we developed a fluorescence detection and stimulation system consisting of a multimode optical fiber used both for delivering the excitation light and for collecting the emitted fluorescence signals.

RESULTS

Slow Oscillation-Associated Population Ca^{2+} Waves In Vivo

For the detection of slow oscillation-associated Ca^{2+} network spikes, we devised an optical fiber-based approach, allowing for the excitation of Ca^{2+} indicator Oregon green 488 BAPTA-1 (OGB-1), the collection of emission light, and the stimulation of ChR2-expressing neurons (Figure 1A). To monitor intracellular Ca^{2+} concentrations, we used the multicell bolus loading technique (Stosiek et al., 2003) in combination with optical fiber-based monitoring of population Ca^{2+} signaling activity (Adelsberger et al., 2005). The tip of the optical fiber (diameter 200 μm) was implanted above the stained cortical or thalamic area (Figure 1B). A column-like region with a diameter of about 400–500 μm in mouse primary visual cortex was stained with OGB-1 (Figure 1C). In conditions of isoflurane anesthesia, slow oscillation-associated population Ca^{2+} transients occurred in the visual cortex at frequencies ranging from 8 to 30 events/min (Figure 1D, see Figure S4E available online), depending on the level of anesthesia (Kerr et al., 2005). It has been shown that Ca^{2+} transients are mediated by Ca^{2+} influx during the spiking activity in a local group of active cortical neurons (Kerr et al., 2005; Rochefort et al., 2009; Stosiek et al., 2003). In line with the previously used terminology (e.g., Rochefort et al., 2009), we refer to these population Ca^{2+} transients as Ca^{2+} waves. Figure 1I shows that spontaneous cortical Ca^{2+} waves are similar to those evoked by visual stimulation (Figure 1E) in terms of amplitude and duration. It is important to note that the comparison of Ca^{2+} wave amplitudes is meaningful only for a given site of optical recording, because the population of Ca^{2+} transients depends on many local parameters, including the level of Ca^{2+} indicator inside cells and the intensity of the excitation light.

Previous work has provided evidence that slow oscillations are initiated in the cortex (Sakata and Harris, 2009; Sanchez-Vives and McCormick, 2000; Timofeev and Steriade, 1996). To obtain deeper insights into the process of slow-wave initiation and propagation, we implemented an optogenetic approach. First, we used a transgenic Thy-1-ChR2 mouse line that expresses ChR2 in layer 5 neurons of the neocortex (Figure 1F) (Arenkiel et al., 2007). When applying a single brief (50 ms) pulse of blue light through the optical fiber (Figure 1G) placed in the visual cortex, we obtained a reliable initiation of Ca^{2+} waves (Figure 1H). Light stimulation in C57/Bl6 mice failed to induce Ca^{2+} waves. Spontaneous, visually evoked, and optogenetically evoked Ca^{2+} waves recorded at a given cortical location had similar waveforms (Figure 1I) and virtually identical duration times and amplitudes (Figures S2A and S2B). The latencies of the onset of Ca^{2+} waves evoked by visual stimulation are quite similar to those evoked by brief (50 ms) optogenetic stimulation (Figure 1J). However, with shorter stimuli, optogenetically induced Ca^{2+} waves occur at longer latencies (Figure 1K). Not too surprisingly, Ca^{2+} waves can be evoked optogenetically not only in visual cortex (Figure S1A) but also in other cortical areas such as the frontal cortex (Figure S1B). Under similar conditions of optogenetic stimulation (a single 50 ms pulse, 73 mW/mm^2), the Ca^{2+} waves that were induced in these two cortical regions had similar waveforms (Figures S1A and S1B) and occurred at similar latencies (90 ± 4 ms VC, 98 ± 5 ms FC).

In order to verify independently that Ca^{2+} waves can be generated in a local group of layer 5 neurons, we expressed ChR2 almost exclusively in a small region within layer 5 of the visual cortex using viral transduction (Figures 2A and 2B). Mice expressed ChR2-mCherry 10 days after virus injection with the expression remaining strong for at least 7 months (Sohal et al., 2009). Viral expression was quantified by serial confocal imaging (see Experimental Procedures). The transduced cortical regions had diameters of 1–1.2 mm. The average number of transfected neurons in the central portion of the virally transduced cortical area, which is the region that was used for optical stimulation, was 215 ± 35 (n = 5 mice), within a sphere of 250 μm radius, which is the average volume of activation under our stimulation conditions (see Supplemental Experimental Procedures and Figure S5). As in transgenic mice, optogenetic stimulation of the virally transduced mice resulted in a reliable initiation of

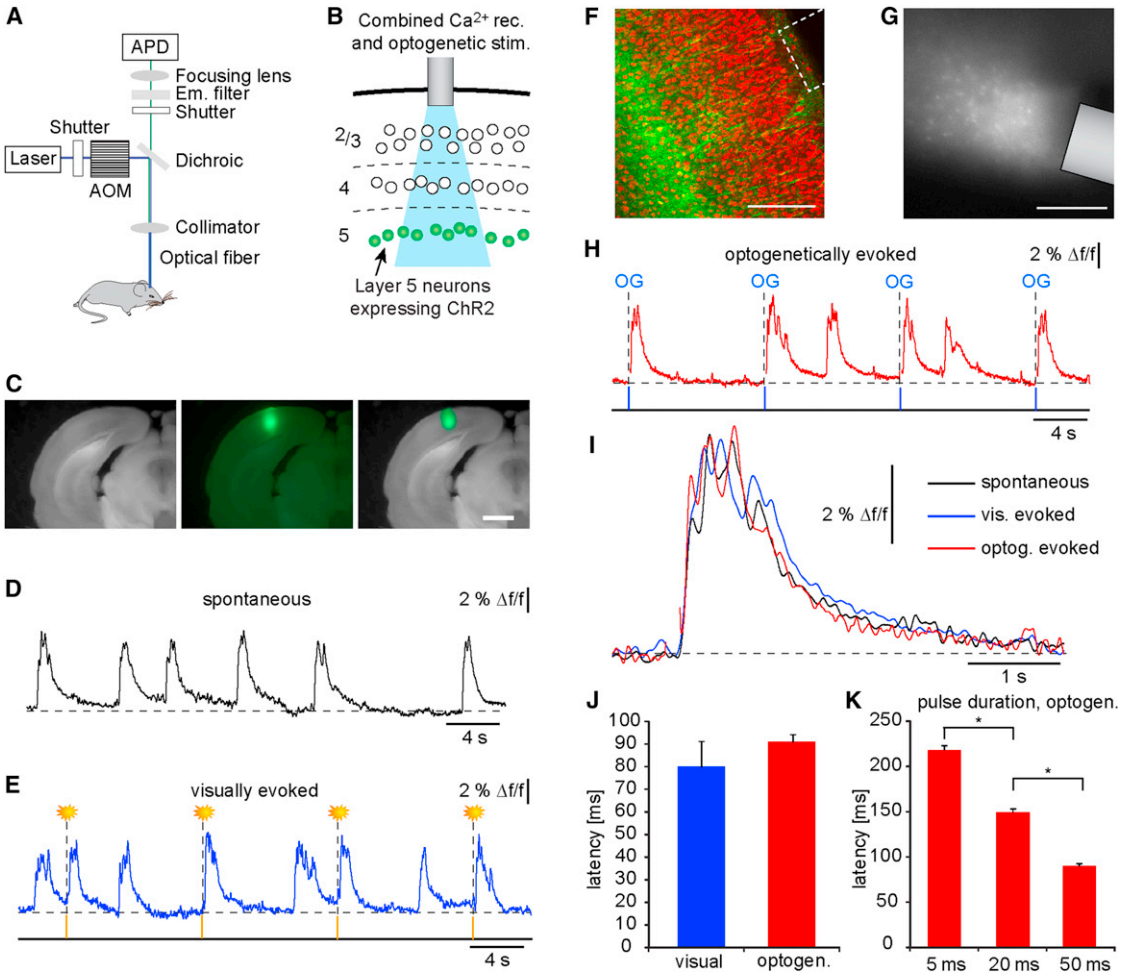

Figure 1. Spontaneous, Sensory-Evoked and Optogenetically Evoked Ca^{2+} Waves in Mouse Visual Cortex

(A) Scheme of the optical fiber recording and stimulation setup. AOM, acousto optic modulator; APD, avalanche photo diode; Em, emission.

(B) Schematic showing the tip of an optic fiber implanted into a stained cortical region above neurons expressing ChR2 (green).

(C) Photomicrographs of a coronal brain slice at the level of the visual cortex (scale bar represents 1 mm). Left: transmitted light only; middle: green fluorescence channel showing the Oregon green 488 BAPTA-1 AM-(OGB-1) stained region; right: overlay.

(D) Spontaneous Ca^{2+} waves in the visual cortex of the anesthetized mouse.

(E) Ca^{2+} waves recorded in the primary visual cortex evoked by a 50 ms light flash applied to both eyes.

(F) Confocal image ex vivo from a fixed section reveals expression of ChR2-YFP in layer 5 neurons in coronal brain slice of Thy-1-ChR2-YFP transgenic mouse (green). Neuronal nuclei are stained with neurotrace (red) (scale bar represents 200 μm). Optical fiber for ChR2 activation and simultaneous Ca^{2+} fluorometric recordings is delineated.

(G) Confocal imaging of OGB-1-stained cortical slice. Only light emitted by fiber was used for OGB-1 excitation (scale bar represents 200 μm).

(H) Ca^{2+} waves evoked by optogenetic stimulation of ChR2-expressing layer 5 neurons of a Thy1-ChR2 transgenic animal. Light pulses of 488 nm wavelength and 50 ms duration, 73 mW/mm^2 light density at tip of fiber.

(I) Overlay of spontaneous, visually evoked, and optogenetically evoked Ca^{2+} waves.

(J) Latencies of slow-wave initiation upon visual (red) versus optogenetic (blue) stimulation, pulse duration = 50 ms. No significant differences were observed, mean ± SEM.

(K) Latencies of optogenetic slow-wave initiation depending on the pulse duration. Latencies differ significantly, in an inverse relation to increasing the pulse duration, mean ± SEM ($p < 0.01$, two-tailed t test).

Ca^{2+} waves (Figure 2C). However, due to the smaller cell number and weaker levels of ChR2 expression compared with transgenic mice, the light pulse duration needed to be increased to 200 ms. Ca^{2+} waves occurred with a latency of 338 ± 12 ms and had a reliability of occurrence of 70% ± 15%. To assess the minimal number of neurons initiating a wave, we titrated down the number of transduced neurons by injecting small quantities of virus solution. We found that optogenetic activation of as few as 60 neurons suffices to evoke a slow wave (Figures 2D and 2E). Together, these experiments establish that Ca^{2+} waves can be effectively triggered by optogenetic activation of a local cluster of layer 5 cortical neurons.

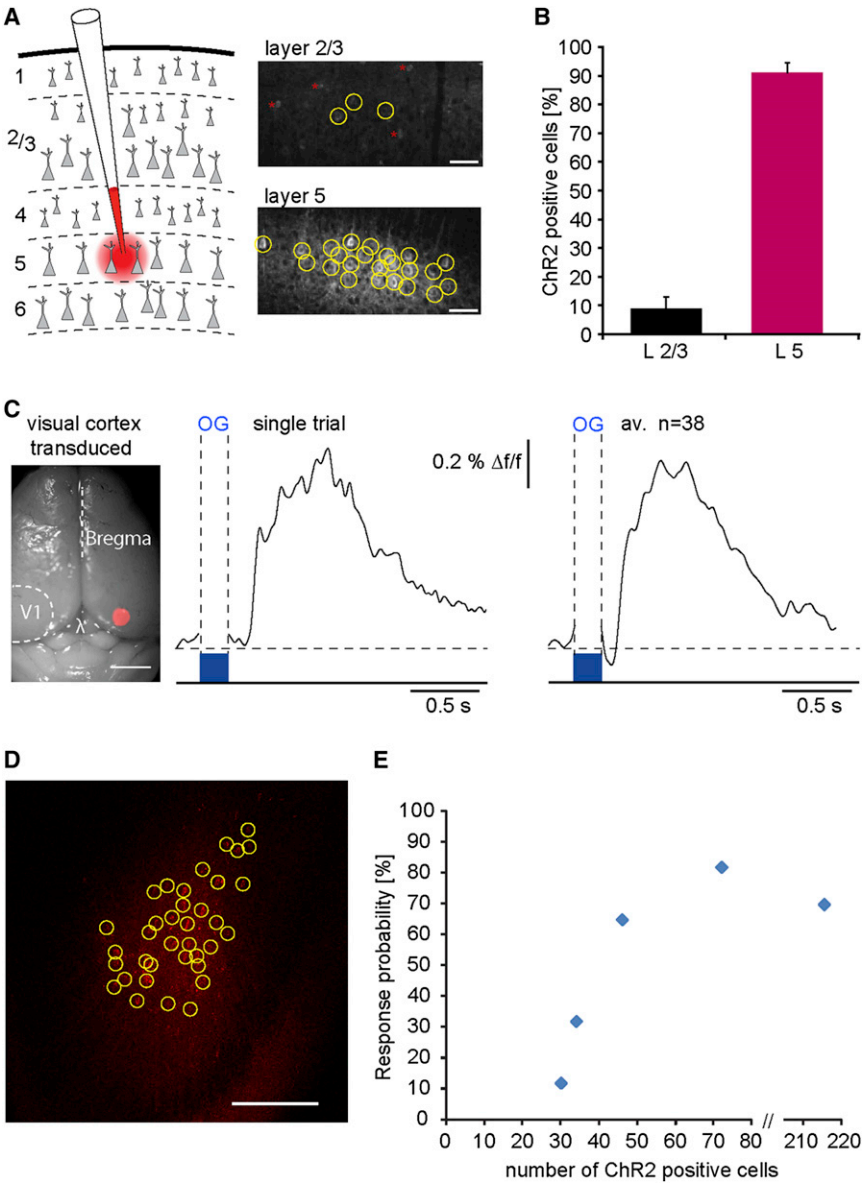

Figure 2. Ca^{2+} Waves Initiated by Single-Pulse Optogenetic Activation of a Local Group of Layer 5 Cortical Neurons

(A) Schematic of viral injection procedure into layer 5 of visual cortex, with confocal images of fixed slices 10 days after viral injection (ChR2-mCherry-AAV). Expression of ChR2-mCherry detected predominantly in cortical layer 5; clearly positive neurons are marked by yellow circle. Red stars mark most likely dendrites. Note that a few neurons in upper cortical layers express ChR2 at low expression levels (scale bar represents 50 μm).

(B) Quantification of relative proportion of ChR2-expressing neurons in layer 2/3 and layer 5, 32 confocal slices, 4 animals, mean ± SEM. No notable expression in other cortical layers could be found.

(C) Photomicrograph of whole brain excluding the bulbus, expression of AAV-ChR2-mCherry in primary visual cortex of the right hemisphere only. Overlay of transmitted light image with red fluorescence channel (scale bar represents 2 mm). Stimulation of virally transduced ChR2-expressing cells in visual cortex with 200 ms light pulses reliably initiates Ca^{2+} waves, single trial and averaged response.

(D) Confocal micrograph of an animal injected with low amount (<50 nl) of virus in layer 5 of visual cortex. Coronal slice, thickness 80 μm, and z projection of 30 optical sections with 2 μm optical thickness are shown; scale bar represents 200 μm. Identified ChR2-positive neurons are marked with a yellow circle. A total number of 46 ChR2-mCherry-expressing neurons can be detected in three coronal slices.

(E) Correlation of response probability of optogenetic induction of slow waves in four animals injected with small virus volumes, resulting in 30–80 ChR2-expressing cells. Pulse duration = 200 ms; detection of slow waves was obtained by ECoG recordings. Rightmost data point: response probability of optogenetic initiation of Ca^{2+} waves of animals injected with larger viral volumes (350 nl, experiments displayed in C), with an average of 215 ± 35 ChR2-positive neurons within the area of activation (n = 5 animals).

Depth-Resolved Local Field Potentials of Optogenetically and Visually Evoked Activity

To determine the electrical correlate of the Ca^{2+} waves, we conducted depth-resolved LFP recordings in Thy1-ChR2-transgenic mice expressing ChR2 in layer 5 (Figure 3). Visual stimulation with a 50 ms light pulse to both eyes resulted in a primary neuronal response that was followed by a secondary slow wave. The fast primary response was most prominent at depths ranging from 300–500 μm (Figure 3A), in line with an initial strong activation of layer 4, while the largest amplitudes of the slow-wave component were found at depths larger than 800 μm, corresponding to layers 5 and 6 (Figures 3A and 3C). The latencies of the visually evoked electrically recorded slow waves are comparable to those of the corresponding Ca^{2+} waves (Figure S2C), showing a trend toward shorter latencies. By comparison, short light pulses (5 ms) in transgenic Thy-ChR2 mice led to a fast short-latency primary response in all cases detected in all cortical layers, which was followed by a subsequent secondary slow wave (Figures 3B and 3D). The latencies of slow-wave emergence are in good agreement with the latencies observed in our Ca^{2+} recordings (Figure S2D). Furthermore, a similar latency between the optogenetically evoked fast and slow components was found when using electrocorticogram (ECoG) recordings (Figures S2E and S2F). Finally, the depth profile of LFP amplitudes was remarkably similar for visually evoked (Figure 3E), optogenetically evoked (Figure 3F), and spontaneous slow waves (Figure 3G), in line with the high degree of similarity of the corresponding Ca^{2+} wave activity (Figures S2A and S2B).

Next, we asked whether the optogenetic initiation of Ca^{2+} waves is restricted to the stimulation of layer 5 or whether

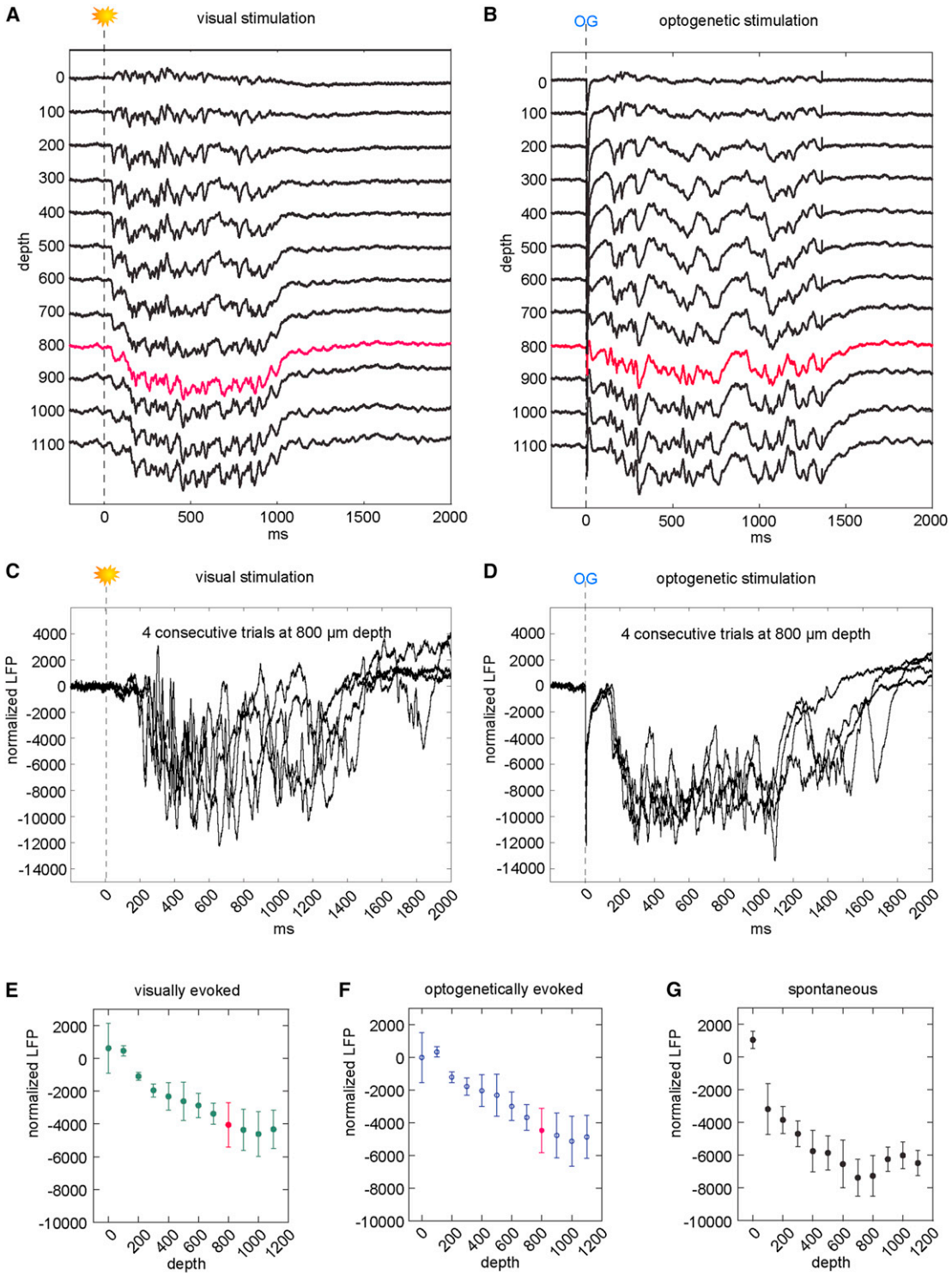

Figure 3. Depth-Resolved LFP Recordings of Slow-Wave Activity upon Visual and Optogenetic Stimulation

Recordings obtained with a multisite electrode (12 recording sites, distance between electrodes 100 µm) implanted in visual cortex of Thy1-ChR2 transgenic mice.

(A) Visual stimulation with light flash of 50 ms duration at time point 0. Fast response with short latency was followed by evoked wave.

(B) Mouse stimulated with 5 ms pulse of blue light at time point 0 ms. Fast primary response was followed by secondary slow wave.

(C and D) LFP recordings at 800 µm cortical depth, corresponding to the red traces in (A) and (B). Four consecutive trials are displayed upon visual stimulation (C) or optogenetic stimulation (D) at time point 0.

(E–G) Depth profile of amplitude of visually evoked (E), optogenetically evoked (F), and spontaneous slow wave (G), mean ± SEM.

stimulation of the upper cortical layers is also effective. For this purpose, we used identical viral constructs and virus titers and targeted the injection of ChR2-mCherry AAV mixed with AAV-cre to layer 2/3 of mouse visual cortex (Figure S3A). We found good expression of ChR2-mCherry 10 days after injection in the upper layers, mostly layer 2/3, that we assessed by confocal imaging (n = 4 animals, 28 confocal slices). In addition, we also detected some expression of ChR2 in neurons in layer 5 (<20% of all ChR2-positive neurons) but at rather low expression levels (Figures S3A and S3B). Notably, in these conditions, optogenetic stimulation completely failed to evoke Ca^{2+} waves, even using maximal light intensities, pulse durations of up to 200 ms, and larger diameter optical fibers (400 μm) (Figure S3C). This result was confirmed by depth-resolved LFP recordings, in which we detected only the primary short-latency response in the upper cortical layers, the sites of strong ChR2 expression, but not the slow-wave component (Figure S3D).

All-or-None Behavior and Refractoriness of Cortical Ca^{2+} Waves

Ca^{2+} waves can be optogenetically evoked with surprisingly short light pulses (Figures 4A–4D). While pulse lengths of 2 ms were ineffective, even 3 ms pulses could evoke Ca^{2+} waves, albeit with a low probability (about 10%, Figure 4D). With longer pulse lengths, the probability increased gradually, reaching nearly 100% for durations of more than 50 ms (Figure 4D). Ca^{2+} waves occurred in an all-or-none manner with remarkably constant amplitudes despite the varying duration of the stimulation pulses (Figures 4A and 4B), at least when stimulated at low frequencies (see below). For a given pulse length, the probability of wave induction decreased when decreasing the intensity of the excitation laser light. Figures 4E and 4F illustrate results showing that, for 50 ms pulses, the response probability changed linearly with the laser power. The all-or-none behavior indicates that the optogenetic stimulation induces an effective activation of the network in which, typically, a similar total number of neurons is activated from trial to trial. Previous two-photon Ca^{2+} imaging recordings indicate that in the sparsely active mature cortex, at least in layer 2/3, a fraction of about 10%–15% of the neurons are active during each wave in the adult rodent, depending on the developmental stage (Golshani et al., 2009; Kerr et al., 2005; Rochefort et al., 2009).

Another remarkable feature of the Ca^{2+} waves was that their induction was suppressed when they were shortly preceded by another Ca^{2+} wave (Figures 4G and 4H). The specific nature of the preceding wave (spontaneous, sensory evoked, or optogenetically evoked) was not a determining factor. In analogy to repetitively evoked action potentials in neurons, induction of Ca^{2+} wave was refractory at short time intervals. Thus, during the initial 1.5 s period after the onset of the first spontaneous Ca^{2+} wave, neither visual nor optogenetic stimulation evoked a wave, demonstrating total refractoriness. A relative refractoriness was encountered during the interval of 1.5–3 s, during which waves with smaller amplitudes were evoked. At intervals longer than 3 s, the subsequent Ca^{2+} waves had normal amplitudes and waveforms (Figure 4I).

Intracortical Propagation of Ca^{2+} Waves

Both spontaneous and sensory-evoked slow oscillatory events are believed to propagate in the cortex (Ferezou et al., 2007; Massimini et al., 2004; Xu et al., 2007). However, many features of this propagation, including the cortical range of propagation and the role of the thalamus, are not entirely understood. Here, we explored the propagation of Ca^{2+} waves by using recordings with multiple fibers implanted at various locations of the cortex and/or thalamus and by using a modified approach to high-speed cortical surface Ca^{2+} imaging. Figure 5 illustrates experiments in which we implanted two optical fibers at different cortical sites after staining those regions with OGB-1. In the experiment shown in Figure 5A, the two fibers were located in the frontal and the visual cortex of the same hemisphere. We noted that spontaneous Ca^{2+} waves occurring at these two remote sites were highly correlated. However, the order of activation changed randomly, with the waves occurring first either in the frontal cortex (Figure 5B, leftmost) or in the visual cortex (Figure 5B, rightmost) and sometimes almost simultaneously in both regions (Figure 5B, middle). There was a significantly higher probability of the waves occurring first in the frontal cortex (64% ± 6%, n = 4 mice), which becomes apparent in the distribution of relative latencies (Figure 5C). This finding is consistent with human studies showing that spontaneous waves of activity recorded by EEG travel predominantly from frontocentral to parietal/occipital cortical areas (Massimini et al., 2004). Figure 5D shows recordings of spontaneous activity obtained in the visual cortices of the two hemispheres and illustrates the high correlation of Ca^{2+} wave activity. In this case, Ca^{2+} waves were first detected at the two recordings with nearly the same probability (48% first in left hemisphere, 52% first in right hemisphere, n = 3 mice).

Next, we explored the cortical propagation of both sensory-evoked and optogenetically evoked Ca^{2+} waves. Figure 5E shows an experiment in which the optical fibers were placed in the frontal and in the visual cortex. Upon presentation of the stimulation light flash, Ca^{2+} waves were reliably evoked in the visual cortex. After their occurrence in the visual cortex, corresponding Ca^{2+} waves were invariably detected also in the frontal cortex, where they occurred with a relative latency of 80 ± 6 ms (392 waves, 7 animals). Figures 5F and 5G show experiments in which Ca^{2+} waves were evoked at various cortical sites by local optogenetic stimulation. In the experiment shown in Figure 5F, the optogenetic stimulation of the visual cortex evoked Ca^{2+} wave activity that was recorded in the visual, frontal, and contralateral frontal cortices at an increasing latency. Similar results were obtained in six out of six experiments. Figure 5G provides quantitative information on the latencies of Ca^{2+} wave initiation and propagation to various cortical locations. Thus, the optogenetic stimulation of V1, with a 50 ms light pulse, evoked a Ca^{2+} wave in V1 within 90 ± 4 ms (14 animals) (Figure 5GI), the time period required for the local buildup of wave activity. Stimulation in V1 generated a Ca^{2+} wave in the ipsilateral FC after 172 ± 5 ms (9 animals) (Figure 5GII) and in the contralateral FC after 204 ± 8 ms (6 animals) (Figure 5GIII). Similar latencies were noted when Ca^{2+} waves were recorded in V1 upon optogenetic stimulation in the ipsilateral FC (Figure 5GV) or the contralateral FC (Figure 5GVI). Together, these results indicate that different

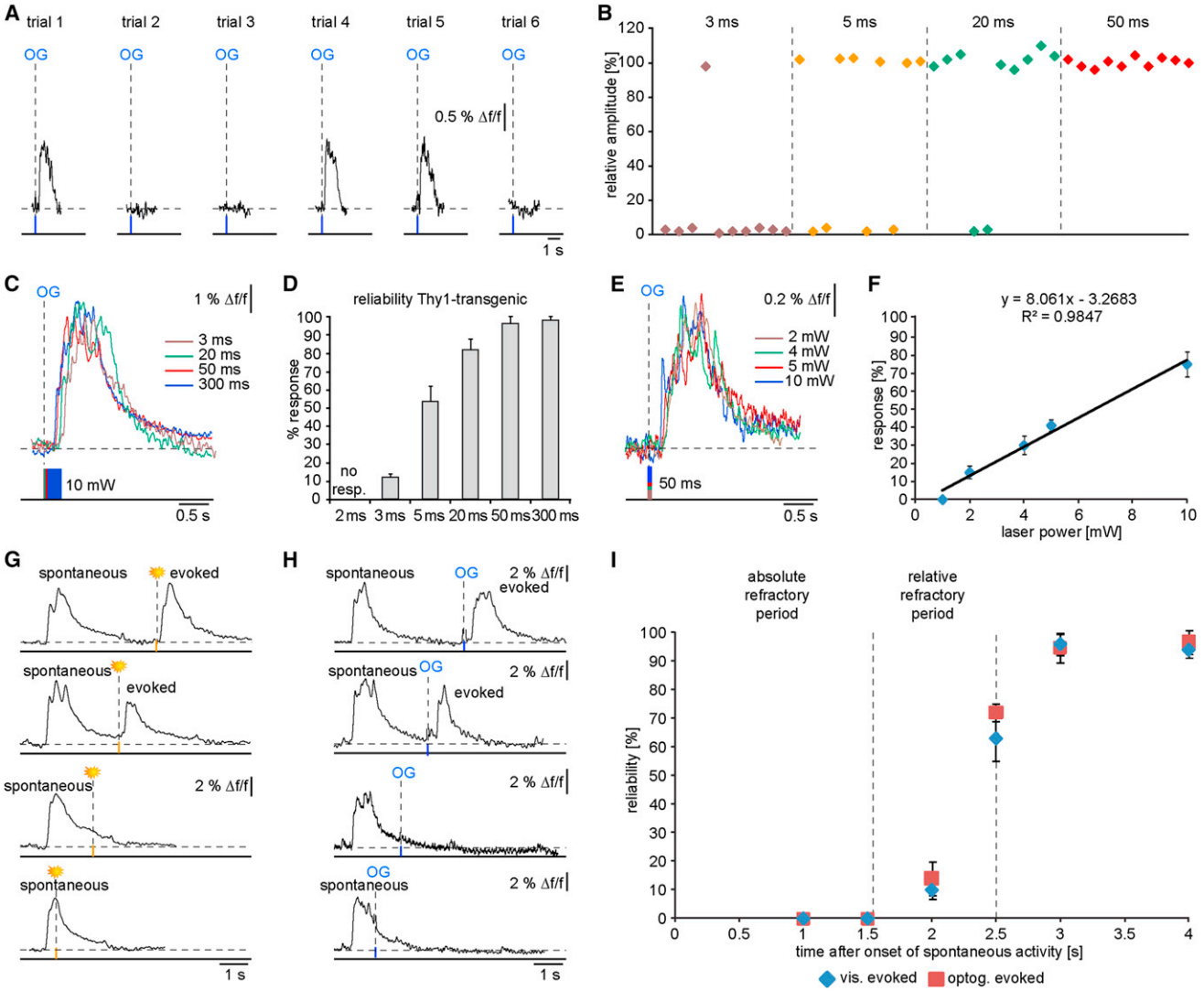

Figure 4. All-or-None Behavior and Refractoriness of Ca^{2+} Waves

(A) Optogenetic stimulation with 5 ms pulse duration; six subsequent trials are displayed. Recordings were obtained in the visual cortex of Thy1-ChR2 transgenic mice.

(B) Quantification of maximum fluorescence amplitudes in a time window of 1 s after light pulses of different pulse lengths, ten single trials each. Fluorescence intensity is normalized to the average amplitude of Ca^{2+} waves.

(C) Overlay of waves evoked by light pulses of varying duration, 10 mW (73 mW/mm^2) laser power.

(D) Summary data on the probability of Ca^{2+} wave initiation depending on duration of light pulse, mean ± SEM. n = 5 experiments, 120 trials in each category.

(E) Overlay of waves upon optogenetic stimulation with 50 ms light pulse and varying light intensities.

(F) Dependency of the probability of response on laser power, mean ± SEM. Linear fit results in an R^2 of 0.985.

(G) Visual stimulation of both eyes with 50 ms light pulses in decreasing temporal distance to spontaneous Ca^{2+} wave. Within 2.5 s upon onset of spontaneous wave, visual stimulation cannot evoke a subsequent wave.

(H) Optogenetic stimulation by applying a 50 ms light pulse to primary visual cortex of transgenic Thy-1 mouse. Again, within 2.5 s, optogenetic stimulation fails to evoke a subsequent wave.

(I) Summary data on refractoriness of Ca^{2+} waves. Probability of initiation versus time after onset of spontaneous wave, mean ± SEM.

neocortical regions, including V1, FC, and possibly all other cortical areas, can generate Ca^{2+} waves that can recruit remote cortical sites.

To test that the locally evoked population Ca^{2+} transient is indeed a propagating wave, we devised a high-speed camera-based approach to record fluorescence signals from large cortical areas (Figure 6A). By multiple injections of OGB-1, we first stained a larger cortical area with dimensions of about 1–2 by 4–5 mm (Figures 6B and 6C). We then monitored changes in Ca^{2+} concentration that occurred at the cortical surface by imaging at 125 frames/s. We found that visual stimulation produced a Ca^{2+} signal that emerged locally at the

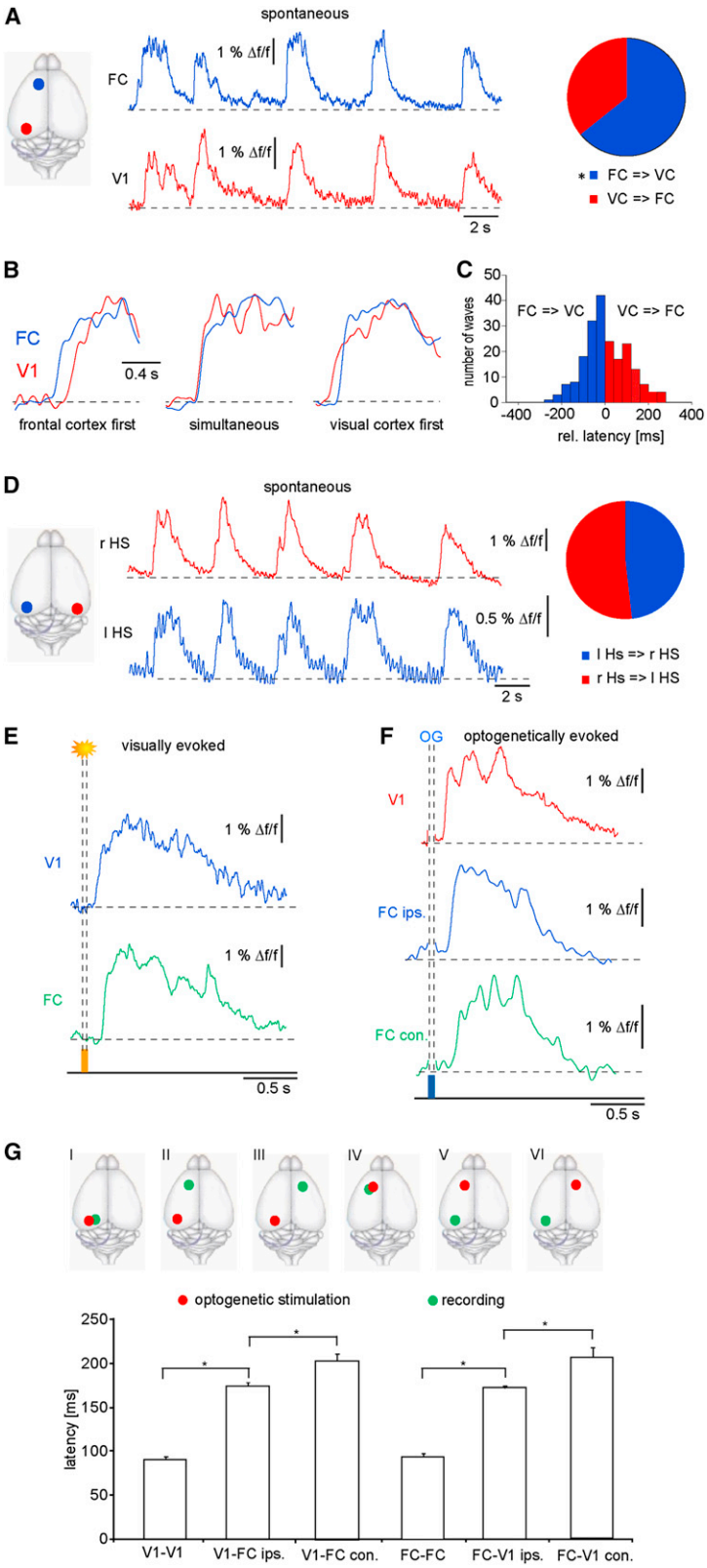

Figure 5. Widespread Cortical Propagation of Ca^{2+} Waves

(A) Two-fiber recordings in visual (red) and frontal (blue) cortex. We recorded 64% ± 6% of all waves in frontal cortex first (n = 4 animals, 204 waves). χ^2 test results in a significant deviation from equal distribution (50:50; $p < 0.01$).

(B) Temporal correlation of onsets of waves, recorded in frontal cortex first (leftmost), almost simultaneously (middle), or in visual cortex first (rightmost).

(C) Frequency histogram on the relative latencies of wave recordings in frontal or visual cortex (n = 4 animals, 204 waves).

(D) Two-fiber recordings in right (red) and left (blue) hemisphere. We recorded 48% of waves first in left hemisphere and 52% in the right hemisphere; 243 waves in n = 3 experiments.

(E) Two-fiber recordings in visual (blue) and frontal (green) cortex upon visual stimulation by applying light flashes (50 ms) to both eyes. Visually evoked Ca^{2+} waves are always recorded in visual cortex first, and with some delay, in the frontal cortex.

(F) Optogenetic stimulation in visual cortex, 50 ms light pulse duration. Recordings in visual cortex, left hemisphere (red), frontal cortex left (blue), and right (green) hemisphere, are shown.

(G) Stimulation of ChR2-expressing layer 5 neurons of transgenic animals in visual cortex (I, II, and III) and frontal cortex (IV, V, and VI); recording in ipsi- (I and V) and contralateral (VI) visual cortex and ipsi- (II and IV) and contralateral (III) frontal cortices. Latencies upon onset of Ca^{2+} waves depend on recording location, mean ± SEM. Latencies differ significantly when comparing recording sites ($p < 0.01$, two-tailed t test).

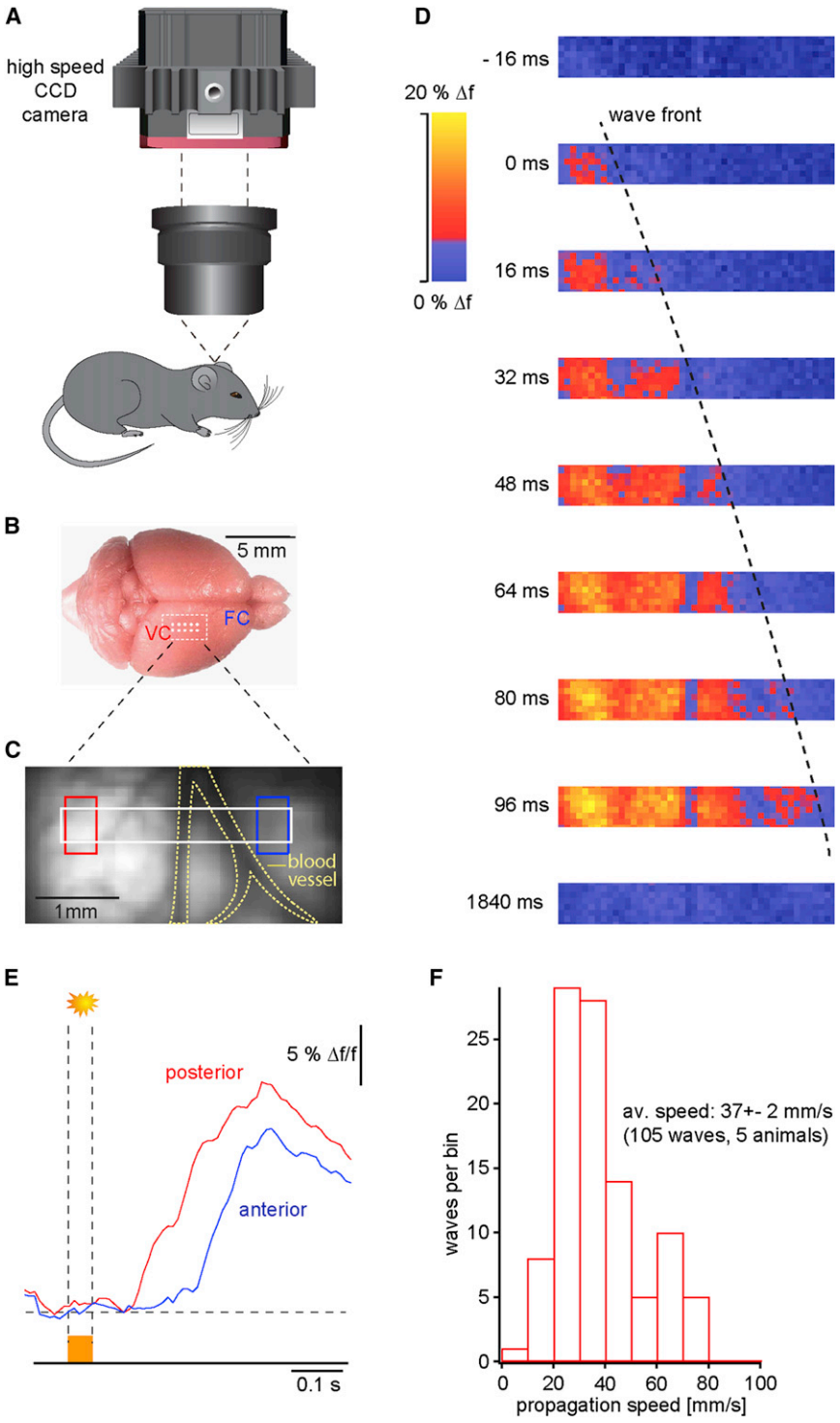

Figure 6. Visualization of the Wave Front of Cortical Ca^{2+} Waves

(A) High-speed CCD-based camera setup allows for recording of large cortical areas in vivo.

(B) Micrograph of mouse brain overlayed with scheme delineating area of OGB-1 injections.

(C) Fluorescence image obtained with CCD camera, recorded with a frequency of 125 Hz. Regions of interest (ROIs) are delineated (white, wave front analysis; red and blue, propagation speed analysis).

(D) False color images of fluorescence emission; 0 ms is defined as onset of Ca^{2+} wave; wave front is delineated. After 1,840 ms, the fluorescence emission returned to baseline.

(E) Time course of the onset of visually evoked Ca^{2+} waves. Transient of anterior ROI, red (see C); posterior ROI, blue.

(F) Histogram of propagation speeds of Ca^{2+} waves recorded by high-speed CCD camera.

visual cortical surface and then gradually propagated toward the frontal cortex (Figure 6D). Propagation in other directions within the skull-covered cortex most likely also took place but could not be monitored. The "wave front" of the Ca^{2+} transient usually did not form a crisp border but often consisted of active hotspots, indicating that local sites of increased activity preceded the main Ca^{2+} wave. This notion is also supported by the observation that the rise times of the Ca^{2+} transients were relatively slow, ranging between 100–200 ms (Figure 6E). The superposition of the Ca^{2+} transients recorded in the posterior and the anterior portion of the cortex, respectively, indicates the latency of wave occurrence at the remote cortical site (Figure 6E). From such latencies we calculated the speed of Ca^{2+} wave propagation (Figure 6F) and found that, on average, Ca^{2+} waves propagated at 37 ± 2 mm/s (105 waves, 5 animals). Comparable values (48 ± 7 mm/s, 9 animals) were obtained when deducing the speed from two-point measurements with optical fibers.

Investigation of Thalamic Ca^{2+} Waves

The optic fiber-based approach is not only useful for cortical recordings but represents one of the few optical techniques that allows access to deeper brain areas such as the thalamus. To test whether slow oscillation-associated Ca^{2+} waves also occur in the thalamus, we stained the dorsolateral geniculate nucleus (dLGN) with OGB-1 and implanted an optical fiber with its tip located in the dLGN (Figure 7A). Upon visual stimulation, we detected Ca^{2+} waves in the dLGN that were tightly temporally correlated with the light stimulus (Figure 7B). Notably, upon light stimulation and implantation of a second optical fiber in the visual cortex, Ca^{2+} waves were invariably first detected in V1 and only after a delay of more than 200 ms in the dLGN (Figures 7C and 7D).

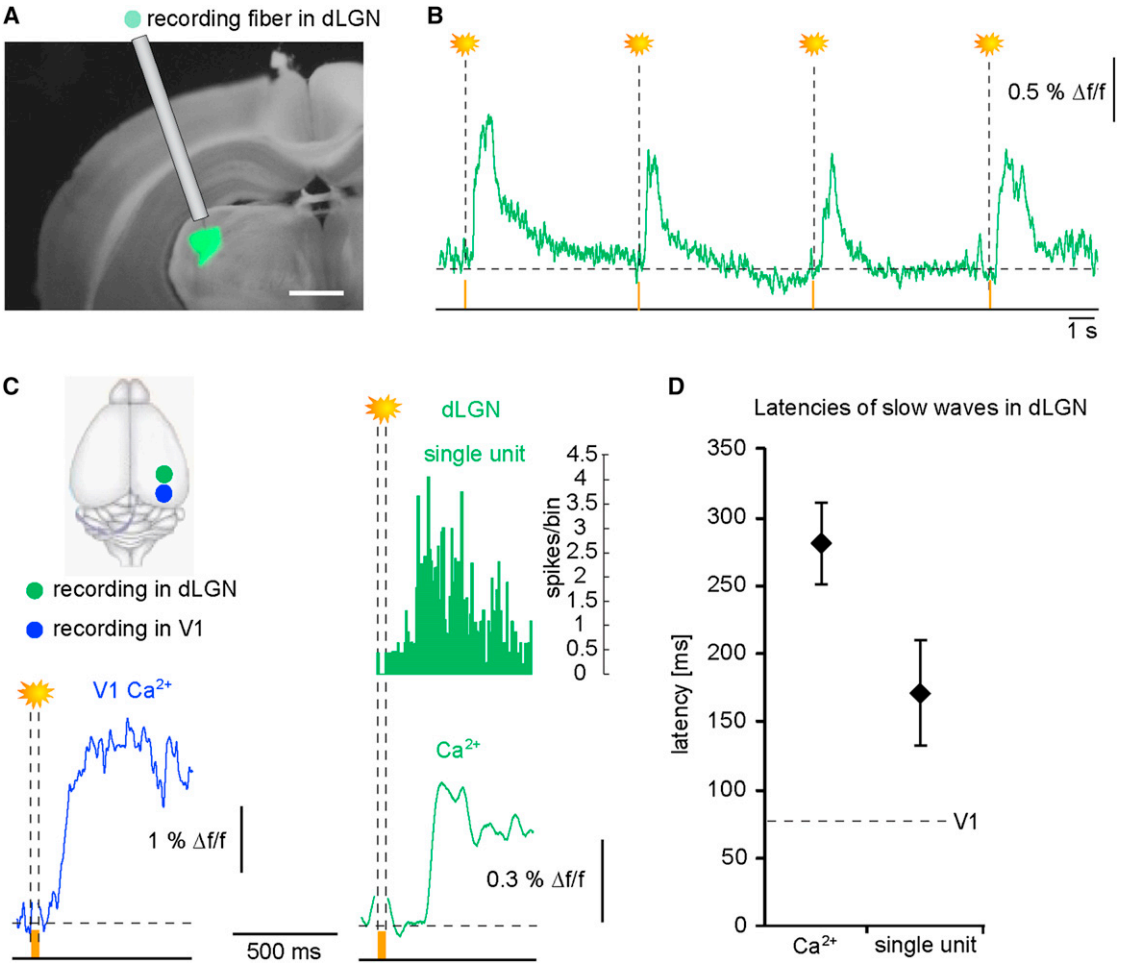

Figure 7. Identification of Thalamic Ca^{2+} Waves

(A) Overlay of transmitted light micrograph of coronal brain slice with green fluorescence channel upon staining with Ca^{2+} indicator OGB-1 in dLGN (scale bar represents 1 mm).

(B) Thalamic Ca^{2+} waves recorded in dLGN evoked by a 50 ms light flash applied to both eyes of the anesthetized mouse.

(C) Simultaneous fiber recordings in visual cortex and dLGN and separate single-unit recordings in dLGN. For single-unit recordings, 90–190 trials per animal (n = 4) were used to construct individual poststimulus spike histogram (PSTH). The average single-unit PSTH is shown from four dLGN neurons together with a representative Ca^{2+} wave from another experiment (right). The Ca^{2+} wave on the left (blue) was recorded simultaneously with the thalamic one (green trace on the right).

(D) Average latencies of the onsets of light-evoked Ca^{2+} waves (n = 210, 6 animals) and light-evoked single-unit activity in thalamic neurons (n = 4 neurons in 4 mice, mean ± SEM).

This indicates that the early afferent thalamic response is carried by a small number of neurons, which do not produce a Ca^{2+} response that can be detected by optical fiber recordings. Instead, slow Ca^{2+} waves, which engage a large proportion of cortical and thalamic neuronal populations, can be readily detected by optical fiber recordings. These Ca^{2+} waves correspond to the slow oscillation-related electrical neuronal events in the thalamus that were previously reported by others (He, 2003; Timofeev and Steriade, 1996). We found that in thalamic neurons, the increase in spiking rate occurred with latencies ranging from 130 to 225 ms (mean 168 ms) after the visual stimulus (Figures 7C and 7D). The longer latencies that were observed for the corresponding thalamic Ca^{2+} waves (Figures 7C and 7D) may be explained, at least in part, by the slower kinetics and the reduced sensitivity of Ca^{2+} recordings, as well as the slower and more variable buildup of wave activity in the thalamus.

This interpretation was supported by experiments in which we used a transgenic Thy-1 mouse line that expresses ChR2 not only in the cortex but also in the thalamus, including the dLGN (Arenkiel et al., 2007) (Figure 8A). By using thalamic ChR2 stimulation, we found again that Ca^{2+} waves were first detected in V1 and only with a delay of 180–200 ms in dLGN (Figures 8B and 8C). Furthermore, a third optical fiber that was inserted in the OGB-1-stained ipsilateral ventral-posterior-medial nucleus (VPM) detected the Ca^{2+} wave activity after an even longer delay (Figure 8C). It is important to note that in using optic fiber-based population Ca^{2+} recordings we did not detect any

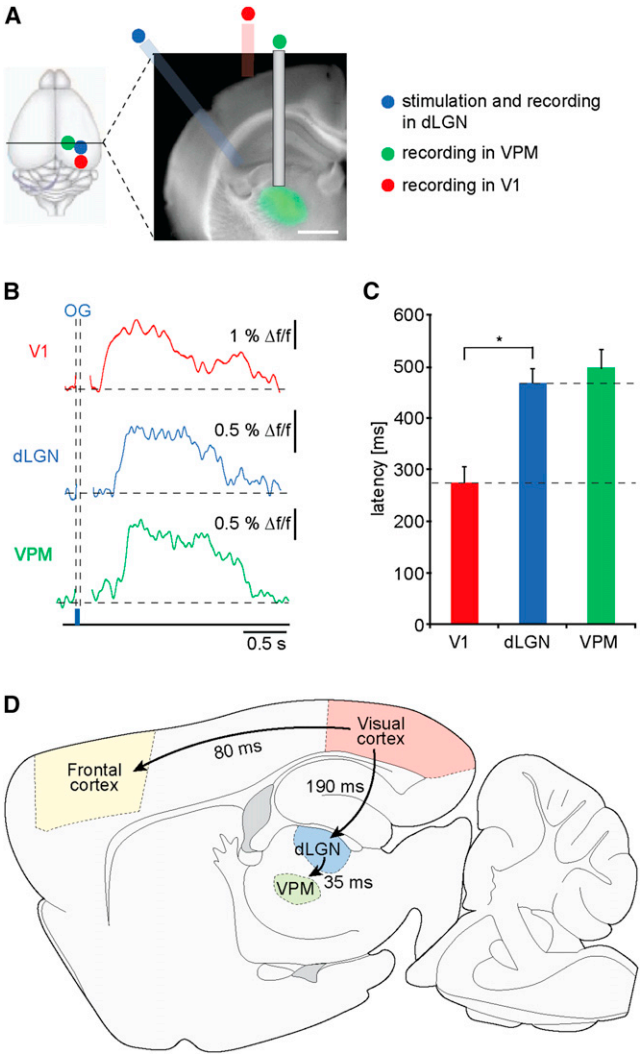

Figure 8. Thalamic Ca^{2+} Waves Strictly Follow Cortical Ca^{2+} Waves

(A) Photomicrograph of staining of VPM with OGB-1 (scale bar represents 1 mm). Stimulation and recording sites are schematically illustrated. Thalamic optogenetic stimulation with pulse durations of 50 ms was conducted in transgenic mice.

(B) Optogenetic stimulation in dLGN and recording of Ca^{2+} waves in dLGN, VPM, and visual cortex (V1). Ca^{2+} waves can be reliably initiated by intrathalamic stimulation, always being recorded in visual cortex first.

(C) Latencies of wave onset upon thalamic stimulation, mean ± SEM. Latencies of Ca^{2+} wave onsets in visual cortex are significantly shorter than in dLGN and VPM ($p < 0.01$, two-tailed t test, $n = 6$ experiments, 192 waves).

(D) Scheme illustrating global propagation of optogenetically induced Ca^{2+} waves.

short-latency responses from the ChR2-expressing thalamic neurons, which are activated within a few milliseconds upon light illumination (Boyden et al., 2005). This may indicate that a small number of thalamic neurons, which do not produce a Ca^{2+} signal that can be detected by fiber recordings, is sufficient for the induction of cortical Ca^{2+} waves.

Figure 8D summarizes our main results concerning the initiation and propagation of slow oscillation-associated Ca^{2+} waves. First, we indicate that Ca^{2+} waves are initiated in the cortex. Second, we show that Ca^{2+} waves travel even to remote cortical sites within 80–100 ms. By contrast, even the recruitment of the nearest thalamic site, such as the dLGN for V1, requires more than 190 ms.

DISCUSSION

In this study, we used a combined optogenetic stimulation and optical recording approach to analyze slow Ca^{2+} waves in the neocortex and thalamus. In comparison to electric recordings of population activity (Kajikawa and Schroeder, 2011), optical recordings are spatially better defined, enabling the study of the local cortical initiation and long-range propagation of slow oscillation-associated Ca^{2+} waves with a higher precision. Furthermore, combining optic recordings with optogenetic stimulation allows for probing the causality between the spatiotemporal activation of distinct cortical and/or thalamic circuits and slow oscillation-associated Ca^{2+} waves. Here, by using these optical approaches, we find that optogenetically evoked Ca^{2+} waves share close similarities with spontaneous and sensory-evoked Ca^{2+} waves and, therefore, represent a useful tool for the analysis of general properties of slow cortical oscillations. We obtained the following major results: (1) optogenetic stimulation of a local cluster of about 100 cortical pyramidal layer 5 neurons for as brief as 3 ms is sufficient to evoke a Ca^{2+} wave; (2) the analysis of these Ca^{2+} waves revealed surprising features of slow oscillation-associated events that were not found in previous studies using electrical recordings, namely that single events exhibit an all-or-none behavior and a marked refractoriness; and, finally, (3) we demonstrate that Ca^{2+} waves propagate through the cortex at a speed of about 37 mm/s and that the recruitment of the thalamus is secondary to the generalized cortical wave activity.

Activation of Layer 5 Pyramidal Neurons Is Sufficient for the Generation of Ca^{2+} Waves

There is accumulating evidence that slow-wave oscillations are of cortical origin. Experimental support for this notion came already from the pioneering work of Steriade and colleagues (Steriade et al., 1993c; Timofeev and Steriade, 1996), demonstrating the persistence of cortical slow oscillations in vivo in thalamically lesioned cats. Similarly, a recent study also using thalamic lesions obtained analogous results in rodents (Constantinople and Bruno, 2011). Furthermore, studies performed by McCormick and colleagues in acute cortical slices of the ferret as well as a recent study in the cat in vivo suggested a dominating role of layer 5 in the generation of slow oscillations (Chauvette et al., 2010; Sanchez-Vives and McCormick, 2000). In line with these observations, Harris and colleagues reported that sensory-evoked wave activity in vivo is first observed in deep cortical layers (Sakata and Harris, 2009). These findings are further supported by our additional experiments expressing ChR2 in layer 2/3 and failing to evoke Ca^{2+} waves (Figure S3).

The role of the thalamus for wave propagation and initiation is not well understood. Despite the above-mentioned evidence indicating that slow waves are initiated in the cortex, there is also evidence suggesting that the thalamus may play a key

role for the generation of slow oscillations in the intact brain, requiring the interplay between two intrinsic thalamic oscillators and one cortical oscillator (Crunelli and Hughes, 2010). These authors argued that there is a need for in vivo studies in nonlesioned animals. In line with their suggestion, we now explored slow-wave activity in nonlesioned animals. Previous work by others using two-photon Ca^{2+} imaging (Kerr et al., 2005; Sawinski et al., 2009), as well as earlier studies using voltage-sensitive dye imaging (Ferezou et al., 2007; Xu et al., 2007), had demonstrated the power of optical techniques for the analysis of slow-wave (or Up-Down state) activity. Here we used optic fiber-based Ca^{2+} recordings (Adelsberger et al., 2005) and a modified approach to Ca^{2+} imaging in vivo using a charge-coupled device (CCD) camera for the analysis of slow-wave activity.

Our results demonstrate that optogenetic stimulation of a local cluster of layer 5 neurons reliably evokes slow oscillation-associated Ca^{2+} waves. Due to the spatial specificity of optogenetic stimulation, we rule out that the thalamus is involved in the early phase of Ca^{2+} wave initiation. The conclusions are based on three lines of evidence: (1) local stimulation produced robust wave activity in transgenic mice expressing ChR2 in layer 5 of the cortex, (2) similarly, stimulation also reliably induced Ca^{2+} waves when ChR2 was expressed exclusively in a local cluster of layer 5 neurons of the visual cortex upon viral transduction, and (3) thalamic stimulation (dLGN) in transgenic mice produced Ca^{2+} waves that were initiated in V1. Notably, we were capable of optogenetically inducing Ca^{2+} waves in different cortical areas, including the frontal and the visual cortices; hence, we conclude that the capacity to induce global Up states is a widespread property of cortical layer 5 neurons.

Cortical Dominance for Corticothalamic Ca^{2+} Wave Initiation and Propagation

Propagation of sensory-evoked, Up state-associated neuronal activity in restricted cortical regions has been previously shown in studies using voltage-sensitive dye imaging (VSDI) (Ferezou et al., 2007; Luczak et al., 2007). There is evidence that, at least in the visual cortex, waves can have spiral-like patterns (Huang et al., 2010). Furthermore, it has been shown that propagation of Up state-associated events occurs even in reduced cortical preparations, like brain slices (Ferezou et al., 2007; Luczak et al., 2007; Sanchez-Vives and McCormick, 2000; Xu et al., 2007). However, the patterns of wave propagation on a larger scale in vivo, with an intact thalamus, were not entirely clear. In humans, EEG studies indicated that spontaneous slow oscillations have a higher probability of initiation in frontocentral cortical areas (Massimini et al., 2004), followed by a propagation toward parietal/occipital areas. These results are consistent with our present observations of spontaneous Ca^{2+} wave behavior, indicating a higher probability of wave initiation in the frontal as compared to the visual cortex. As shown previously with VSDI for electrical events, we now demonstrate that Ca^{2+} waves propagate continuously through the cortex, recruiting large areas, perhaps even the entire cortex. In contrast to studies applying VSDI (Huang et al., 2010), we did not observe spiral or other nonlinear wave patterns. A possible explanation for this discrepancy may be that VSDI reflects primarily subthreshold activity, whereas Ca^{2+} imaging using fluorescent dyes mainly reflects suprathreshold neuronal activity (Garaschuk et al., 2006b; Lütcke et al., 2010; Rochefort et al., 2009).

The first field potential recordings of thalamic slow-wave oscillations were obtained in hemidecorticated cats in vivo (Timofeev and Steriade, 1996). In that study, the authors provided evidence from a small sample of combined cortical EEG and thalamic field potential recordings that spontaneous cortical waves preceded the associated thalamic ones. In the present study, we determined the corticothalamic wave latencies only for sensory- and optogenetically evoked waves, because these have, unlike spontaneous waves, a defined, unique site of cortical initiation. For such evoked waves, we demonstrate a clear temporal dominance of cortical over the thalamic wave initiation. Thus, visually evoked Ca^{2+} waves as well as Ca^{2+} waves evoked by intrathalamic optogenetic stimulation occur first in the visual cortex and only after a delay of about 180–200 ms in the dLGN. We emphasize that our findings only apply to the slow-wave activity. The primary fast neuronal activation upon visual stimulation will take place in the visual thalamic nuclei first, before being transmitted to the thalamorecipient cortical layer 4.

Ca^{2+} Waves Reflect "Windows of Opportunity" for Long-Range Corticothalamic Integration

Irrespective of their mode of initiation, Ca^{2+} waves were found to be remarkably unitary with virtually constant amplitudes and durations at a given brain location. This suggests that during waves of different origins, including the spontaneous, sensory-evoked, or optogenetically induced ones, a similar number of neurons participates on average in the slow oscillatory activity. Our results obtained using optical Ca^{2+} recordings reveal properties of the slow oscillatory events that were not recognized previously. First, we observed an all-or-none behavior of the Ca^{2+} waves. The analysis of the optogenetically evoked waves particularly demonstrated that light pulses as short as 3 ms either evoke a full wave or no wave at all. Similarly, different light intensities for a given duration of the stimulating light pulse either evoked a full wave or no wave at all. Second, repetitive stimulation allowed the induction of consecutive waves only for intervals that were longer than about 2.5 s. For shorter intervals, wave initiation was either partially or, for very short intervals, completely refractory. Finally, locally initiated waves travel over long distances through both brain hemispheres. Together, these observations support the idea that, at least under the conditions of anesthesia, sleep, or perhaps quiet wakefulness (Poulet and Petersen, 2008), activity that is generated locally in a small cortical area can spread over long distances and recruit large corticothalamic regions into an event that has a unitary character. During a period, lasting for about a second, a large group of neurons throughout most of the cortex and thalamus is coactive during an Up state. On average, the number of neurons that are active during the Up state appears to be largely constant. These observations assign a new meaning to the notion that Up states represent "windows of opportunity" for cortical signaling (Compte et al., 2008), by identifying network Ca^{2+} waves as stereotypic periods of global corticothalamic recruitment in vivo, during which locally

generated neuronal activity is transmitted and computed in large-scale circuits.

EXPERIMENTAL PROCEDURES

Virus Injection

All experiments were carried out according to institutional animal welfare guidelines and were approved by the government of Bavaria, Germany. Adult C57/Bl6 mice were anesthetized with an intraperitoneal bolus injection of a mixture of ketamine and xylazine and placed in a stereotaxic frame. Above the primary visual cortex (V1), a craniotomy was made 3.8 mm posterior to bregma and 2.0 mm lateral to the midline. Viral constructs were delivered through a small durotomy by a glass micropipette with an outer tip diameter of 45 μm and an inner diameter of 15 μm. The micropipette was slowly inserted 600 μm below the pia for targeting of cortical layer 5 and 100 μm for targeting of layer 2/3. Two adeno-associated virus (AAV) preparations, serotype 2, were mixed at a ratio of 1:4: AAV-CAG-Cre and AAV-EF1A-DIO-hChR2(H134R)-mCherry. We injected 350 nl of the viral solution into V1 at a rate of 0.1 μl/min (Cardin et al., 2009). After the injection, the pipette was held in place for 5 min before slowly retracting it from the brain. The scalp incision was closed with tissue adhesive (Vetbond, 3M Animal Care Products), and postinjection analgesics were given to aid recovery. Optical recordings were carried out after a minimum of 10 days after viral construct injection.

Histology and Confocal Imaging

For characterization of ChR2 expression, animals were perfused transcardially with 4% PFA 10 days postinjection and the brains were postfixed for 24 hr. We cut 70- to 80-μm-thick sections with a vibratome (Leica), stored them in PBS, and mounted them in Vectashield (Vector Laboratories) containing media for confocal imaging. Tissue sections were analyzed with an Olympus Fluoview confocal microscope (FV 1000) equipped with 20× (oil) and 10× objectives (UPlanSAPO, Olympus), with numerical apertures of 0.85 and 0.4, respectively.

Recording and Stimulation Set-Up

A custom-built set-up was used for combined optical fiber-based optogenetic stimulation and neuronal Ca^{2+} recordings (Figure 1A). Close correlation of optically recorded Ca^{2+} waves and ECoG transients could be demonstrated, proving that the optical set-up is suitable in detecting slow oscillation-associated Ca^{2+} waves (Figures S4A and S4B). For details, see Supplemental Experimental Procedures.

Staining with Fluorescent Ca^{2+} Indicator and Optical Fiber Recordings and Stimulations

C57/Bl6 as well as Thy1-ChR2 transgenic mice aged between postnatal day 20 (P20) and P40 were anesthetized by isoflurane (Abbott) at concentrations between 0.8% and 1.5% in pure O_2. From then on, the animals were kept at a constant depth of anesthesia, characterized by a loss of reflexes (tail pinch, eye lid) and respiration rates of 80–100 breaths per minute. A small craniotomy was made above the respective cortical or thalamic area; for details, see Supplemental Experimental Procedures. The coordinates of the craniotomy were as follows: for primary visual cortex (V1) (from bregma): AP −3.8 mm, ML 2 mm (relative to midline); frontal cortex: AP 3 mm, ML 1 mm, dLGN: AP −2 mm, ML 2 mm; and VPM: AP −1.75, ML 1.2. The injection solution containing OGB-1 was prepared as described in Garaschuk et al. (2006a) and Stosiek et al. (2003). We filled 5 μl of the dye-containing solution into a patch pipette and inserted 300 μm for all cortical stainings, 2.5 mm for dLGN, and 3.5 mm for VPM. Approximately 1–2 μl of the staining solution were injected into the brain. About 30 min after dye application, the fiber tip was inserted into the stained region with a micromanipulator to the depth, providing maximal fluorescence intensity, typically at 100 μm below the cortical surface. For thalamic recordings, the optical fiber was inserted according to the DV coordinates used for staining, and insertion was halted a minimum of 100 μm above staining depth to avoid lesion of stained area. All recordings were obtained in conditions in which the cortex and thalamus were in a continuously oscillatory state, producing regularly recurring slow oscillation-associated Ca^{2+} waves.

Optogenetic and Visual Stimulation

For visual stimulation, light flashes with durations of 50 ms were delivered to both eyes of the mouse by two white LEDs (SLSNNWH812TS, Samsung) with a light power of 0.12 mW each. A light-dense cone was used to confine visual stimulation light to the eyes. Optogenetic stimulation was conducted at varying laser power levels ranging between 1 and 10 mW. Light power at the tip of the fiber was linearly dependent on the output laser power, ranging between 7.3 mW/mm^2 and 73 mW/mm^2. Pulse duration and power levels were controlled by custom-written software in LabView and applied via a PCI 6731 (National Instruments) AD/DA converter. Time marks at the start of each stimulus were recorded together with the continuous fluorescence waveform for offline analysis. For the analysis of typically activated neurons in the Thy-1 transgenic animals, see Supplemental Experimental Procedures.

Electrical Recordings

For recordings of the epidural electrocorticogram, two silver wires (0.25 mm diameter; insulated except the nodular ends) were implanted epidurally.

Depth-resolved LFPs were recorded with a 16 channel probe (Neuronexus probe model: A1X16-3mm-100-177, Neuronexus). For in vivo juxtasomal cortical and thalamic recordings, 4.5 to 5.5 MΩ patch pipettes pulled from borosilicate filamented glass were used. For details, see Supplemental Experimental Procedures.

CCD Camera Recordings

For CCD camera recordings, a head chamber made from a plastic dish with a central opening was glued onto the skull after removing the skin. To obtain a large cranial window, the cranium was thinned with a dental drill to form a rectangle with the dimensions of about 4 × 2 mm. Subsequently, the thinned cranium was lifted with a thin injection needle (30G) with the aid of a dissecting microscope. Specific staining of the exposed brain area with OGB-1 was achieved by multiple multicell bolus loading. Throughout the entire experiment the head chamber was perfused with ringer solution containing 125 mM NaCl, 4.5 mM KCl, 26 mM $NaHCO_3$, 1.25 mM NaH_2PO_4, 2 mM $CaCl_2$, 1 mM $MgCl_2$, and 20 mM glucose (pH 7.4) and bubbled with 95% O_2 and 5% CO_2. The set-up for CCD camera-based detection of Ca^{2+} waves consisted of a low-magnification fluorescence microscope (MacroView MVX10, Olympus) equipped with a highly sensitive CCD camera (NeuroCCD, Redshirt Imaging) mounted on top. Images were recorded at an acquisition rate of 125 Hz and using custom-made LabView software (National Instruments).

Postrecording Documentation and Data Processing

At the end of each experiment, the animal was sacrificed through inhalation of pure CO_2. Brains were removed and images were taken before and after slicing to document the exact position of the staining and recording region. Images were obtained using a PCO pixelfly CCD camera (pco.imaging) mounted on an upright microscope (Zeiss Axioplan, Carl Zeiss) or a dissection microscope. Fluorescent images were acquired using a YFP or mCherry filter set and overlaid with the transmitted light images.

The analysis of Ca^{2+} traces was performed using the Igor software (WaveMetrics). All traces represent relative changes in fluorescence (Δf/f), after subtraction of background. The Ca^{2+} baselines were determined by analyzing the corresponding amplitude histograms. For each transient, a linear slope was fitted between 10% and 50% of the peak amplitude of the wave. The intersection of the linear slope and the baseline was then identified as the onset of that transient, and latencies were calculated from the time of initiation of light pulses to the onset of the wave. For all optogenetic experiments, the light artifact during stimulation pulses was omitted from the traces. The analysis of latencies of electric slow waves in depth-resolved LFP recordings was conducted at a cortical depth of 800 μm. The fluorescence images acquired by the CCD camera were color coded by assigning to the baseline the color blue. The cut-off between blue and the warm colors corresponds to the minimal response. A response was accepted if its amplitude exceeded two times the value of the root mean square of the baseline signal.

Statistical Analysis

Statistical analysis was conducted using SPSS software. First, data sets from all conditions were tested for normal distribution using the parameter-free

one-sample Kolmogorov-Smirnov test (Young, 1977). In cases in which normal distribution of data could be assumed ($p > 0.05$), the parametric two-tailed Student's t test was employed to compare means. For testing the statistical significance of the deviation of the proportion of values compared to equal distribution, the χ^2 test was applied. A p value of $p < 0.05$ was considered significant.

SUPPLEMENTAL INFORMATION

Supplemental Information includes five figures and Supplemental Experimental Procedures and can be found with this article online at http://dx.doi.org/10.1016/j.neuron.2013.01.031.

ACKNOWLEDGMENTS

The authors thank Jia Lou for help with preparing the figures, Sarah Bechtold and Rosa Karl for virus preparation, Rebecca Mease for help with data analysis, Rita Förster for perfusion of mice, and the other laboratory members for critical comments on the manuscript. This work was supported by the Friedrich Schiedel Foundation and by the European Commission under the 7th Framework Programme, Project Corticonic. S. Fischer and C. Rühlmann were supported by the DFG (IRTG 1373). A. Konnerth designed the study. A. Stroh and C. Rühlmann performed the viral construct injections and confocal imaging. A. Stroh, C. Rühlmann, A. Schierloh, and H. Adelsberger performed the optical fiber recordings. S. Fischer and H. Adelsberger conducted and analyzed the camera recordings. A. Groh and A. Stroh conducted the electrophysiological measurements. A. Stroh and K. Deisseroth established the optogenetic procedures. A. Konnerth and A. Stroh wrote the manuscript.

Accepted: January 23, 2013
Published: March 20, 2013

REFERENCES

Adelsberger, H., Garaschuk, O., and Konnerth, A. (2005). Cortical calcium waves in resting newborn mice. Nat. Neurosci. *8*, 988–990.

Arenkiel, B.R., Peca, J., Davison, I.G., Feliciano, C., Deisseroth, K., Augustine, G.J., Ehlers, M.D., and Feng, G. (2007). In vivo light-induced activation of neural circuitry in transgenic mice expressing channelrhodopsin-2. Neuron *54*, 205–218.

Boyden, E.S., Zhang, F., Bamberg, E., Nagel, G., and Deisseroth, K. (2005). Millisecond-timescale, genetically targeted optical control of neural activity. Nat. Neurosci. *8*, 1263–1268.

Cardin, J.A., Carlén, M., Meletis, K., Knoblich, U., Zhang, F., Deisseroth, K., Tsai, L.H., and Moore, C.I. (2009). Driving fast-spiking cells induces gamma rhythm and controls sensory responses. Nature *459*, 663–667.

Chauvette, S., Volgushev, M., and Timofeev, I. (2010). Origin of active states in local neocortical networks during slow sleep oscillation. Cereb. Cortex *20*, 2660–2674.

Compte, A., Reig, R., Descalzo, V.F., Harvey, M.A., Puccini, G.D., and Sanchez-Vives, M.V. (2008). Spontaneous high-frequency (10-80 Hz) oscillations during up states in the cerebral cortex in vitro. J. Neurosci. *28*, 13828–13844.

Constantinople, C.M., and Bruno, R.M. (2011). Effects and mechanisms of wakefulness on local cortical networks. Neuron *69*, 1061–1068.

Crunelli, V., and Hughes, S.W. (2010). The slow (<1 Hz) rhythm of non-REM sleep: a dialogue between three cardinal oscillators. Nat. Neurosci. *13*, 9–17.

Doi, A., Mizuno, M., Katafuchi, T., Furue, H., Koga, K., and Yoshimura, M. (2007). Slow oscillation of membrane currents mediated by glutamatergic inputs of rat somatosensory cortical neurons: in vivo patch-clamp analysis. Eur. J. Neurosci. *26*, 2565–2575.

Ferezou, I., Haiss, F., Gentet, L.J., Aronoff, R., Weber, B., and Petersen, C.C. (2007). Spatiotemporal dynamics of cortical sensorimotor integration in behaving mice. Neuron *56*, 907–923.

Gao, L., Meng, X., Ye, C., Zhang, H., Liu, C., Dan, Y., Poo, M.M., He, J., and Zhang, X. (2009). Entrainment of slow oscillations of auditory thalamic neurons by repetitive sound stimuli. J. Neurosci. *29*, 6013–6021.

Garaschuk, O., Milos, R.I., Grienberger, C., Marandi, N., Adelsberger, H., and Konnerth, A. (2006a). Optical monitoring of brain function in vivo: from neurons to networks. Pflugers Arch. *453*, 385–396.

Garaschuk, O., Milos, R.I., and Konnerth, A. (2006b). Targeted bulk-loading of fluorescent indicators for two-photon brain imaging in vivo. Nat. Protoc. *1*, 380–386.

Golshani, P., Gonçalves, J.T., Khoshkhoo, S., Mostany, R., Smirnakis, S., and Portera-Cailliau, C. (2009). Internally mediated developmental desynchronization of neocortical network activity. J. Neurosci. *29*, 10890–10899.

Gradinaru, V., Zhang, F., Ramakrishnan, C., Mattis, J., Prakash, R., Diester, I., Goshen, I., Thompson, K.R., and Deisseroth, K. (2010). Molecular and cellular approaches for diversifying and extending optogenetics. Cell *141*, 154–165.

Grienberger, C., Adelsberger, H., Stroh, A., Milos, R.I., Garaschuk, O., Schierloh, A., Nelken, I., and Konnerth, A. (2012). Sound-evoked network calcium transients in mouse auditory cortex in vivo. J. Physiol. *590*, 899–918.

Haider, B., Duque, A., Hasenstaub, A.R., and McCormick, D.A. (2006). Neocortical network activity in vivo is generated through a dynamic balance of excitation and inhibition. J. Neurosci. *26*, 4535–4545.

Hanganu, I.L., Ben-Ari, Y., and Khazipov, R. (2006). Retinal waves trigger spindle bursts in the neonatal rat visual cortex. J. Neurosci. *26*, 6728–6736.

He, J. (2003). Slow oscillation in non-lemniscal auditory thalamus. J. Neurosci. *23*, 8281–8290.

Huang, X., Xu, W., Liang, J., Takagaki, K., Gao, X., and Wu, J.Y. (2010). Spiral wave dynamics in neocortex. Neuron *68*, 978–990.

Kajikawa, Y., and Schroeder, C.E. (2011). How local is the local field potential? Neuron *72*, 847–858.

Kerr, J.N., Greenberg, D., and Helmchen, F. (2005). Imaging input and output of neocortical networks in vivo. Proc. Natl. Acad. Sci. USA *102*, 14063–14068.

Khazipov, R., Sirota, A., Leinekugel, X., Holmes, G.L., Ben-Ari, Y., and Buzsáki, G. (2004). Early motor activity drives spindle bursts in the developing somatosensory cortex. Nature *432*, 758–761.

Landsness, E.C., Crupi, D., Hulse, B.K., Peterson, M.J., Huber, R., Ansari, H., Coen, M., Cirelli, C., Benca, R.M., Ghilardi, M.F., and Tononi, G. (2009). Sleep-dependent improvement in visuomotor learning: a causal role for slow waves. Sleep *32*, 1273–1284.

Lindén, H., Tetzlaff, T., Potjans, T.C., Pettersen, K.H., Grün, S., Diesmann, M., and Einevoll, G.T. (2011). Modeling the spatial reach of the LFP. Neuron *72*, 859–872.

Luczak, A., Barthó, P., Marguet, S.L., Buzsáki, G., and Harris, K.D. (2007). Sequential structure of neocortical spontaneous activity in vivo. Proc. Natl. Acad. Sci. USA *104*, 347–352.

Lütcke, H., Murayama, M., Hahn, T., Margolis, D.J., Astori, S., Zum Alten Borgloh, S.M., Göbel, W., Yang, Y., Tang, W., Kügler, S., et al. (2010). Optical recording of neuronal activity with a genetically-encoded calcium indicator in anesthetized and freely moving mice. Front. Neural Circuits *4*, 9.

MacLean, J.N., Watson, B.O., Aaron, G.B., and Yuste, R. (2005). Internal dynamics determine the cortical response to thalamic stimulation. Neuron *48*, 811–823.

Massimini, M., Huber, R., Ferrarelli, F., Hill, S., and Tononi, G. (2004). The sleep slow oscillation as a traveling wave. J. Neurosci. *24*, 6862–6870.

McCormick, D.A., Shu, Y., Hasenstaub, A., Sanchez-Vives, M., Badoual, M., and Bal, T. (2003). Persistent cortical activity: mechanisms of generation and effects on neuronal excitability. Cereb. Cortex *13*, 1219–1231.

Poulet, J.F., and Petersen, C.C. (2008). Internal brain state regulates membrane potential synchrony in barrel cortex of behaving mice. Nature *454*, 881–885.

Rigas, P., and Castro-Alamancos, M.A. (2007). Thalamocortical Up states: differential effects of intrinsic and extrinsic cortical inputs on persistent activity. J. Neurosci. *27*, 4261–4272.

Rochefort, N.L., Garaschuk, O., Milos, R.I., Narushima, M., Marandi, N., Pichler, B., Kovalchuk, Y., and Konnerth, A. (2009). Sparsification of neuronal activity in the visual cortex at eye-opening. Proc. Natl. Acad. Sci. USA *106*, 15049–15054.

Rolls, A., Colas, D., Adamantidis, A., Carter, M., Lanre-Amos, T., Heller, H.C., and de Lecea, L. (2011). Optogenetic disruption of sleep continuity impairs memory consolidation. Proc. Natl. Acad. Sci. USA *108*, 13305–13310.

Sakata, S., and Harris, K.D. (2009). Laminar structure of spontaneous and sensory-evoked population activity in auditory cortex. Neuron *64*, 404–418.

Sanchez-Vives, M.V., and McCormick, D.A. (2000). Cellular and network mechanisms of rhythmic recurrent activity in neocortex. Nat. Neurosci. *3*, 1027–1034.

Sawinski, J., Wallace, D.J., Greenberg, D.S., Grossmann, S., Denk, W., and Kerr, J.N. (2009). Visually evoked activity in cortical cells imaged in freely moving animals. Proc. Natl. Acad. Sci. USA *106*, 19557–19562.

Shu, Y., Hasenstaub, A., and McCormick, D.A. (2003). Turning on and off recurrent balanced cortical activity. Nature *423*, 288–293.

Sohal, V.S., Zhang, F., Yizhar, O., and Deisseroth, K. (2009). Parvalbumin neurons and gamma rhythms enhance cortical circuit performance. Nature *459*, 698–702.

Steriade, M. (2006). Grouping of brain rhythms in corticothalamic systems. Neuroscience *137*, 1087–1106.

Steriade, M., and Timofeev, I. (2003). Neuronal plasticity in thalamocortical networks during sleep and waking oscillations. Neuron *37*, 563–576.

Steriade, M., Contreras, D., Curró Dossi, R., and Nuñez, A. (1993a). The slow (< 1 Hz) oscillation in reticular thalamic and thalamocortical neurons: scenario of sleep rhythm generation in interacting thalamic and neocortical networks. J. Neurosci. *13*, 3284–3299.

Steriade, M., Nuñez, A., and Amzica, F. (1993b). A novel slow (< 1 Hz) oscillation of neocortical neurons in vivo: depolarizing and hyperpolarizing components. J. Neurosci. *13*, 3252–3265.

Steriade, M., Nuñez, A., and Amzica, F. (1993c). Intracellular analysis of relations between the slow (< 1 Hz) neocortical oscillation and other sleep rhythms of the electroencephalogram. J. Neurosci. *13*, 3266–3283.

Stosiek, C., Garaschuk, O., Holthoff, K., and Konnerth, A. (2003). In vivo two-photon calcium imaging of neuronal networks. Proc. Natl. Acad. Sci. USA *100*, 7319–7324.

Timofeev, I., and Steriade, M. (1996). Low-frequency rhythms in the thalamus of intact-cortex and decorticated cats. J. Neurophysiol. *76*, 4152–4168.

Vyazovskiy, V.V., Olcese, U., Hanlon, E.C., Nir, Y., Cirelli, C., and Tononi, G. (2011). Local sleep in awake rats. Nature *472*, 443–447.

Wang, X.J. (2010). Neurophysiological and computational principles of cortical rhythms in cognition. Physiol. Rev. *90*, 1195–1268.

Wu, J.Y., Huang, Xiaoying, and Zhang, Chuan (2008). Propagating waves of activity in the neocortex: what they are, what they do. Neuroscientist *14*, 487–502.

Xu, W., Huang, X., Takagaki, K., and Wu, J.Y. (2007). Compression and reflection of visually evoked cortical waves. Neuron *55*, 119–129.

Young, I.T. (1977). Proof without prejudice: use of the Kolmogorov-Smirnov test for the analysis of histograms from flow systems and other sources. J. Histochem. Cytochem. *25*, 935–941.

Zhang, F., Wang, L.P., Brauner, M., Liewald, J.F., Kay, K., Watzke, N., Wood, P.G., Bamberg, E., Nagel, G., Gottschalk, A., and Deisseroth, K. (2007). Multimodal fast optical interrogation of neural circuitry. Nature *446*, 633–639.